Identification and Validation of Genes with Expression Patterns Inverse to Multiple Metastasis Suppressor Genes in Breast Cancer Cell Lines

Natascia Marino[1], **Joshua W. Collins**[1], **Changyu Shen**[2], **Natasha J. Caplen**[3], **Anand S. Merchant**[4], **Yesim Gökmen-Polar**[5], **Chirayu P. Goswami**[6], **Takashi Hoshino**[7], **Yongzhen Qian**[8], **George W. Sledge Jr**[9,*], and **Patricia S. Steeg**[1]

[1]Women's Malignancies Branch, Center for Cancer Research, National Cancer Institute, Bethesda, MD, USA

[2]Department of Biostatistics, Indiana University School of Medicine, Indianapolis, IN, USA

[3]Genetics Branch, Center for Cancer Research, National Cancer Institute, Bethesda, MD, USA

[4]CCRIFX Bioinformatics Core, Advanced Biomedical Computing Center, Leidos Biomed, Frederick, MD, USA

[5]Department of Pathology and Laboratory Medicine, Indiana University School of Medicine, Indianapolis, IN, USA

[6]Center for Computational Biology and Bioinformatics, Indiana University School of Medicine, Indianapolis, IN, USA

[7]Takeda Pharmaceutical Company Ltd, Tsukuba, Japan

[8]Laboratory Animal Sciences Program, SAIC-Frederick, National Cancer Institute, Frederick, MD, USA

[9]Department of Medicine, Indiana University School of Medicine, Indianapolis, IN, USA

Abstract

Metastasis suppressor genes (MSGs) have contributed to an understanding of regulatory pathways unique to the lethal metastatic process. When re-expressed in experimental models, MSGs block cancer spread to, and colonization of distant sites without affecting primary tumor formation. Genes have been identified with expression patterns inverse to a single MSG, and found to encode functional, druggable signaling pathways. We now hypothesize that common signaling pathways mediate the effects of multiple MSGs. By gene expression profiling of human MCF7 breast carcinoma cells expressing a scrambled siRNA or siRNAs to each of 19 validated MSGs (NME1, BRMS1, CD82, CDH1, CDH2, CDH11, CASP8, MAP2K4, MAP2K6, MAP2K7, MAPK14,

Corresponding authors: Patricia S. Steeg, Women's Malignancies Branch, Center for Cancer Research, National Cancer Institute, Building 37/ Room 1126, 37 Convent Drive, Bethesda, MD 20892. Phone: 301-402-2732; Fax: 301-402-8910; steegp@mail.nih.gov. Natascia Marino, Women's Malignancies Branch, Center for Cancer Research, National Cancer Institute, Building 37/ Room 1126, 37 Convent Drive, Bethesda, MD 20892. Phone: 301-594-0701; Fax: 301-402-8910; natasciam28@gmail.com.
*Current address: Stanford University School of Medicine, Paolo Alto, CA, USA

Conflict of interest

The authors declare that they have no conflicts of interest.

GSN, ARHGDIB, AKAP12, DRG1, CD44, PEBP1, RRM1, KISS1), we identified genes whose expression was significantly opposite to at least five MSGs. Five genes were selected for further analysis: PDE5A, UGT1A, IL11RA, DNM3 and OAS1. After stable downregulation of each candidate gene in the aggressive human breast cancer cell line MDA-MB-231T, *in vitro* motility was significantly inhibited. Two stable clones downregulating PDE5A (phosphodiesterase 5A), enzyme involved in the regulation of cGMP-specific signaling, exhibited no difference in cell proliferation, but reduced motility by 47 and 66% compared to the empty vector-expressing cells (p=0.01 and p=0.005). In an experimental metastasis assay, two shPDE5A-MDA-MB-231T clones produced 47–62% fewer lung metastases than shRNA-scramble expressing cells (p=0.045 and p=0.009 respectively). This study demonstrates that previously unrecognized genes are inversely related to the expression of multiple MSGs, contribute to aspects of metastasis, and may stand as novel therapeutic targets.

Keywords

metastasis suppressor genes; metastasis; gene expression profiling; bioinformatics; PDE5A; breast cancer

Introduction

In 2013, an estimated 232,340 new cases of invasive breast cancer were expected to be diagnosed among women and approximately 39,620 women were expected to die from breast cancer in the US [1]. Despite improvements in surgery, radiation and chemotherapy, metastatic disease remains the most common contributor to breast cancer-related mortality [2]. Treatment methods developed by focusing on the primary tumor eventually fail in many cases, and metastatic disease remains incurable. Thus, to increase survival, metastasis prevention and more effective treatments for established metastases are necessary.

The metastasis suppressor gene (MSG) family includes genes that, when re-expressed in a metastatic tumor cell, are able to inhibit the metastatic process without reducing primary tumor size. Often, MSGs are downregulated in the metastatic site compared to the primary tumor [3]. Since the discovery in 1988 of the first metastasis suppressor, NM23-H1 (or NME1), the number of confirmed MSGs has increased to over 30 [3–8]. MSGs are involved in cellular processes such as context-specific cellular proliferation, motility, adhesion, invasion, resistance to apoptosis, and angiogenesis. Understanding the biological mechanisms of the MSGs will be crucial to developing treatments that target this process. To date, studies have almost universally concentrated on one specific MSG, rather than investigating commonalities.

Attempts to therapeutically target MSG pathways have been proposed (reviewed in [9]). The identification of drugs that reactivate silenced MSGs has been reported [10–13]. An inverse correlation approach was successfully used to identify new druggable targets to each of two MSGs, *RHOGDI2* (*ARHGDIB*) and *NM23* [14, 15]. By re-expressing *RHOGDI2* in metastatic bladder cancer cells and identifying transcripts repressed by RHOGDI2 and overexpressed in invasive bladder tumors, Titus *et al* discovered both endothelin-1 and neuromedin-U [15]; atrasentan, an inhibitor of endothelin-1, is a new therapeutic agent. For

NM23-H1, Horak *et al* discovered that *LPAR1* (*EDG2*/*LPA1*), a lysophosphatidic acid receptor, was inversely expressed. Re-expression of *LPA1* overcame NM23-H1 inhibition of motility and metastasis [14, 16]. Pharmacologic LPA1 inhibition resulted in significantly reduced metastasis formation with induction of cancer cell dormancy at the metastatic sites in *in vivo* models [17].

Although MSGs appear to have different cellular localizations and functions, pathway interrelationships and redundancies are beginning to emerge [18, 19]. Berger *et al* described the involvement of three MSGs, *NM23*, *MAP2K4* and *PEBP1* (*RKIP*) in two biochemically interconnected Map kinase signaling pathways, MAPK/ERK and JNK signaling [7]. It is likely that multiple common signaling pathways are used by the MSGs, and that some of these pathways can represent interesting translational targets for the development of anti-metastatic strategies. We present herein a first gene expression analysis of multiple MSGs: *AKAP12* (SSeCKS/GRAVIN) [20], *ARHGDIB* [21], *BRMS*1 [22], *CASP8* [23], *CD44* [24, 25], *CD82* (*KAI-1*) [26, 27], *CDH1* [28, 29], *CDH2* [30], *CDH11* [31], *DRG1* [32], *GSN* [33], *KISS1* [34], *MAP2K4* [35], *MAP2K6* [36], *MAP2K7* [37], *MAPK14* (p38-α) [36], *NME1* (NM23/NDPK), *PEBP1* [38], and *RRM1* [39]. We have identified and validated five genes: *DNM3*, *OAS1*, *IL11RA*, *UGT1A*, and *PDE5A* as having expression patterns inverse to at least five (and up to 11) MSGs. As proof of principle, when the expression of each gene was silenced using shRNAs, *in vitro* motility of MDA-MB-231T cells was decreased. *PDE5A* was upregulated in eight of nineteen siRNA-MSG samples. The stable silencing of *PDE5A* in MDA-MB-231T cells using two different shRNAs reduced experimental metastasis by 47 and 62%, respectively.

Materials and Methods

Cell culture conditions

Human breast cancer cell lines MCF7 and BT474, and immortalized kidney cell line HEK293TN were obtained from ATCC (Manassas, VA). BT474-M1 subline was obtained from MC Hung, MD Anderson Cancer Center, TX [40]. A sub-line of human MDA-MB-231 cells, designated MDA-MB-231T, was used [10]. Cells were cultured in Dulbecco's Modified Eagle Medium (DMEM) (Invitrogen, Grand Island, NY) supplemented with 10% FBS, and antibiotics (100 U/ml penicillin, 100 μg/ml streptomycin; Invitrogen), under a humidified 37°C incubator at 5% CO_2.

Gene silencing

RNAis were purchased from Qiagen (Valencia, CA, Supplementary Table S1) and transfected into MCF7 cell line using Lipofectamine™ RNAiMax (Invitrogen) according to the manufacturer's protocol. Briefly, either 2×10^6 or 1×10^6 cells were plated in 100-mm petri dishes and incubated for either 48 h or 96 h, respectively, with 30 nM siRNAs and 30 μl Lipofectamine RNAiMax. These two time points were chosen in order to analyze both the early (48 h) and late (96 h) effects of the MSGs silencing in terms of alteration in downstream gene expression.

To stably knockdown the target genes' expression in MDA-MB-231T cells, Mission-shRNA (Sigma, St. Luis, MO) were used and insertion into the cells was performed using lentiviral particle production and infection according to the manufacturer's protocol. Briefly, 1×10^6 HEK293TN cells were transfected with 1 µg each of shRNA-MSG plasmids and 2 µl packaging mix (Clontech, Montain View, CA) using 3 µl FuGENE HD transfection reagent (Roche, Indianapolis, IN). After 48 h incubation, the medium containing the newly formed viral particles was collected, filtered with Millex-HV 0.45 µm filters (Millipore, Carrigtwohill, CO) and added to 1×10^6 MDA-MB-231T cells together with 5 µg/ml polybrene solution (Sigma). After 24 h infection, cells were washed with PBS, and DMEM containing 1µg/ml Puromycin (Invitrogen) was added to select the infected cells. The following Mission-shRNA plasmids were used: pLKO (SHC001), NT (SHC216), shPDE5A (TRCN0000048743, TRCN0000048745), shDNM3 (TRCN0000051405, TRCN0000051407), shOAS1 (TRCN0000005007, TRCN0000005009), shUGT1A1 (TRCN0000029530, TRCN0000029531), shUGT1A9 (TRCN0000034655, TRCN0000034656).

Microarray analysis

siRNA-MSG transfected MCF7 cells were collected at 48 h and 96 h using TRIzol Reagent method (Invitrogen). RNA was extracted using RNeasy® mini Kit (Qiagen, Valencia, CA) and DNase I (Qiagen) following manufacturer's instructions.

The RNA concentration was assessed using Nanodrop ND-1000 spectrophotometer (ThermoScientific, Wilmington, DE). RNA quality was measured by calculating RNA integrity number on Agilent 2100 Bioanalyzer (Agilent Technologies, Santa Clara, CA).

Following quantification, 1 µg of total RNA was used for microarray analysis and sent to Affymetrix Core Service (NIH, Frederick, MD) where labeling and hybridization reactions were performed using standard Affymetrix protocols. The platform used was the Affymetrix-Genechip Human Genome-U133_Plus_2.0 Array. Expression values were calculated using Affymetrix GeneChip analysis software MAS 5.0. Microarray data can be obtained via the Gene Expression Omnibus repository, accession no. GSE53668. Probes of selected genes are listed in Table 1 and Supplementary Table S2.

Quantitative Reverse-Transcription-Polymerase Chain Reaction (qRT-PCR)

Expression of MSGs or selected target genes was measured by qRT-PCR. Total RNA was extracted as described above. cDNA was synthesized using iScript™ cDNA synthesis Kit (Bio-Rad, Hercules, CA). One µg total RNA was added to the reaction mix (1 µl iScript reverse trancriptase, 4 µl 5X reaction mix, nuclease-free water to 20 µl final volume). The mixture was incubated at 25°C for 5 min, 42°C for 30 min, 85°C for 5 min and 4°C until use. cDNA (10 ng) was used as template with primers (Sigma, listed in Supplementary Table S3) and SYBR Green (Bio-Rad) for qRT-PCR using an iQ5-detection system (Bio-Rad) following manufacturer's instructions. Expression levels of the genes were normalized to GAPDH levels. Results were analyzed using iQ5-Optical System software (Bio-Rad).

Cloning and gene overexpression

IL11RA cDNA was obtained from pOTB-IL11RA plasmid (ATCC, MGC-2146) and subcloned into a lentiviral pCDH-CMV-MCS-EF1-NEO vector (CD514B-1, System Biosciences, Mountain View, CA) using EcoRI and XhoI restriction sites. Lentiviral particles were prepared as described above and MCF7 cells were infected for 48 h and selected with neomycin (1mg/ml).

Western blot analysis

Protein lysates were prepared as previously reported [16]. Membranes were probed over-night at 4°C with the following rabbit polyclonal antibodies: anti-IL11RA (Santa Cruz Biotechnology, Santa Cruz, CA), anti-UGT1A1 (Abcam, Cambridge, MA), anti-OAS1 (Abcam), anti-PDE5A (Abcam), anti-DNM3 (ProteinTech, Chicago, IL). Mouse anti-β-Actin antibody (Sigma) was used as loading control.

Cell migration assay

Transwell migration assays were performed in Boyden chambers as previously described [16]. Each condition for all cell lines was assayed in triplicate wells and each experiment was performed in triplicate.

Cell proliferation assay

Cellular proliferation was measured by 3-(4,5 dimethylthiazol-2-yl)-2,5-diphenyltetrazolium bromide (MTT) assay. 1,000 cells/well were plated in 96 well plates and grown for 24, 48 and 72 h prior to the addition of 10% MTT (Sigma). After 2 h incubation, MTT was solubilized by addition of 100μl/well of DMSO. Plates were incubated for 30 min at 37°C and read on a SpectraMax M2 plate reader (Molecular Devices, Sunnyvale, CA) at 570 nm.

Experimental Pulmonary Metastasis Mouse Model

Experiments were performed under an approved National Cancer Institute (NCI) Animal Use Agreement. Female six-week-old athymic nude mice were obtained from Charles River Laboratories (NCI-Frederick Animal Production Area, Frederick, MD). 5×10^5 MDA-MB-231T cells were injected into the lateral tail vein of each mouse [10]. A total of 10 mice /experimental group was used. At week 9, mice were sacrificed and lungs collected in Bouin's solution (70% picric acid, 25% Formaldehyde, 5% glacial acetic acid). Surface lung metastatic lesions were counted before paraffin-embedding and sectioning (10μm) the tissues. Hematoxylin and Eosin (H&E) staining was performed to visualize and count the metastatic lesions in each section. To measure proliferation rate in metastasis, lungs were stained with rabbit anti-Ki67 antibody (Vector Laboratories, Burlingame, CA), following manufacturer's protocol.

Bioinformatic and statistical analysis

Differential gene expression analysis of the microarray dataset was performed using R software (http://www.r-project.org). ANOVA method was applied to calculate a t-statistic value for relative difference in gene expression based on permutation analysis. Ingenuity

Pathway Systems (Redwood City, CA; http://www.ingenuity.com) was used to conduct pathway exploration.

The significance of mean comparison was assessed by either Student's *t*-test or Mann Whitney test and considering 95% confidence interval. $P<0.05$ was considered to be significant. Validation of the inverse correlation between the selected genes and MSGs in breast tumor cohort was performed analyzing the microarray expression data from two publicly available datasets downloaded from NCBI GEO: GSE2034 and GSE1456 [41, 42]. The two datasets include 286 and 159 breast cancer patients, respectively. Partek Genomics Suite (http://www.partek.com) was used to perform the statistical analysis. The expression data were median-centered and $\log_2$-transformed for each gene across all samples. For each gene of interest, the expression values were averaged and plotted on a bar chart. A third publicly available dataset was used for the Pearson correlation analysis: GSE26304 [43]. This dataset includes 31 pure DCIS, 36 IDC patients, 42 mixed and 6 normal samples.

Results

Inverse association approach to identify downstream targets to multiple MSGs

Based on the success of previous studies identifying functional, druggable inverse correlates of single tumor or metastasis suppressor genes [14, 15], we hypothesized that genes with expression patterns inverse to that of multiple MSGs exist and could provide functional and therapeutic insights into the metastatic process. For this analysis, each of 19 MSGs was silenced *in vitro* and gene expression profiled. The tumorigenic cell line MCF7 was chosen to study the effect of MSG downregulation on gene expression. The expression of each MSG in MCF7 cell line was first verified using qRT-PCR (Supplementary Fig. 1). Most of the MSGs showed a relatively high expression level with *NME1* having the highest expression and *AKAP12* the lowest expression level of the genes analyzed. Independent transfections of MCF7 cells were performed using two different siRNA sequences targeting each MSG (Supplementary Table S1) or a siNeg-siRNA. RNA was harvested 48 h and 96 h post siRNA transfection and the silencing of each MSG was assessed by qRT-PCR compared to either wild type (wt) or siNeg-siRNA transfected cells (Fig. 1). Because of variability in siRNA-Knockdown efficiencies, especially for poorly expressed genes (CDH2, AKAP12, KISS1), data obtained from the two siRNAs were pooled together. To identify genes differentially expressed following silencing of each MSG, we conducted microarray analysis of RNA samples from both the 48 and 96 h MSG siRNA transfected MCF7 cells and control cells (wt and siNeg-siRNA).

Identification of candidate genes inversely associated to multiple MSGs

Affymetrix HG-U133_Plus_2.0 was chosen for gene expression profiling. This platform allows the analysis of over 47,000 transcripts. A total of 77 gene chips were used to analyze the samples. Differentially expressed genes were defined using a combined analysis of the expression profiles of siRNA transfectants of all nineteen MSGs versus the six control samples (three wt and three siNeg) at both time points. At 48 h, 257 genes and at 96 h, 419 genes were upregulated as compared to control samples with a t-statistic (distance between two samples in units of standard deviation) > 2 and $p<0.01$ (Supplemental Table S4 and S5).

Ingenuity pathway analysis identified 6 major biological functions in common between the upregulated genes at 48 h and 96 h: cell morphology, cell signaling, metabolism, proliferation, development and immune signaling (Fig. 2). Eighteen upregulated genes were selected for further validation based on: a) t-statistic larger than 2 and b) *p-value* smaller than 0.01 in at least one of the two time points.

In vitro validation of the inverse association between selected genes and MSGs

The inverse correlation between the expression of multiple MSGs and the selected candidate genes was validated in an independent set of siRNA-MSGs MCF7 transfections using qRT-PCR. Similar to the microarray analyses, target gene expression in siRNA-MSG and siNeg transfected cells were compared at 48 h and 96 h post siRNA transfection. Upregulation of at least 1.5-fold as compared to the control was observed for *UGT1A, OAS1, DNM3, IL11RA, PDE5A, BCAR4, CA9, WNK3, TXNRD1*, and *MMP16* following silencing of five or more MSGs (Fig. 3, Supplementary Fig. 2). In contrast the upregulation of *LPXN, TARP, APH1B, CXCR7, CYP4V2, SRMS, NRIP3*, and *CNTNAP4* was validated for less than five metastasis suppressor genes (Supplementary Fig. 2).

Five candidate genes (*UGT1A, DNM3, OAS1, IL11RA*, and *PDE5*A) were selected for further analysis based on their *p*-values, their occurrence in common pathways shown in Fig. 2 and drug-target suitability (Table 2). In order to assess their association with cell migration ability, each of these five candidate genes was stably silenced in the aggressive human breast cancer cell line MDA-MB-231T using two specific shRNAs and subsequent cell motility was evaluated (Fig. 4). Validation of shRNA silencing was conducted using western blotting.

UGT1A (UDP-glucoronosyltransferase-1 family) was upregulated at 48 h (t-stat=2.77, *p*=0.01) from the siRNA-MSG transfection in the microarray analysis (Table 1). Using qRT-PCR, UGT1A expression was at least 1.5-fold upregulated by the knockdown of eleven genes (*AKAP12, BRMS1, CD44, CD82, CDH11, DRG1, GSN, MAP2K4, MAP2K6, MAP2K7, PEBP1*) (Fig. 3a). The *UGT1A* locus encodes several isoforms of the UDP-glucoronosyltransferase 1 family of proteins involved in the glucoronidation of xenobiotics and endogenous compounds [44]. The probe set used for the microarray was unable to distinguish between the specific isoforms. Our study focused on *UGT1A1* and *UGT1A9* isoforms as they were expressed in MDA-MB-231T cells (Supplementary Fig. 3) and were previously evaluated in relation to breast cancer [45, 46]. MDA-MB-231T cells were stably transfected with shRNA specifically targeting either *UGT1A1* or *UGT1A9* (Fig. 4a). Western blot analysis showed UGT1A1 downregulation in two MDA-MB-231T cell clones, #30 and 31. UGT1A9 downregulation in the two stable clones (#55 and 56) was evaluated using qRT-PCR due to low expression in this cell line. Although the transfection of the shRNA scramble (NT) caused a minor reduction in UGT1A1/9 expression as compared to the empty vector expressing cells (pLKO), cell migration of these two controls was not affected. Motility assays showed a significant reduction in cell migration of clones expressing shUGT1A1 (64 %, *p*=0.003 and 71 %, *p*=0.0004) and shUGT1A9 (56 %, *p*=0.004 and 86 %, *p*=0.001) as compared to the control cells (Non-target, NT). No difference in cell proliferation was observed (Supplementary Fig. 4a).

DNM3 encodes Dynamin-3, a member of a family of GTPases associated with microtubules and involved in vesicular transport and endocytosis [47]. DNM3 was also upregulated at 48 h (t-stat=2.52, *p*=0.01) following the silencing of MSG genes (Table 1). Validation by qRT-PCR showed at least a 1.5-fold upregulation of *DNM3* following silencing of six MSGs (*CASP8, CD44, CD82, CDH1, GSN, MAP2K4*) (Fig. 3b). The stable silencing of DNM3 (clones #05 and 07; Fig. 4b) showed a trend in reduced cell migration compared to control shRNA (NT) expressing cells (36.4 %, *p*=0.046 and 30.3 %, *p*=0.2, respectively). No difference in cell proliferation was observed (Supplementary Fig. 4b).

OAS1 (2′-5′-Oligoadenylate Synthetase-1) encodes a member of the 2–5 synthetase family involved in the innate immune response to viral infection [48]. This gene was upregulated at 48 h (t-stat=2.82, *p*=0.01) and at 96 h (t-stat=2.88, *p*=0.01) from the siRNA-MSG transfection in the microarray analysis (Table 1). The qRT-PCR validation experiment showed at least a 1.5-fold OAS1 upregulation by six MSGs (*ARHGDIB, CD44, CD82, CDH11, MAP2K4, MAP2K7*) (Fig. 3c). After transfection of two shRNAs targeting OAS1, the two stable clones #07 and 09 showed a reduction in OAS1 expression by Western blot and a trend in reducing cell motility as compared to the NT cells (26.5 %, *p*=0.02 and 32 %, *p*=0.08 respectively) (Fig. 4c). No difference in cell proliferation was observed (Supplementary Fig. 4c).

IL11RA encodes the α – subunit that, together with gp130, forms IL11 receptor [49]. It was upregulated in the microarray analysis at 48 h (t-stat=2.18, *p*=0.04) and at 96 h (t-stat=5.69, *p*<0.001) from the siRNA-MSG transfections (Table 1). The qRT-PCR validation showed at least a 1.5-fold increase of *IL11RA* expression upon knockdown of eleven MSGs (*ARHGDIB, BRMS1, CDH1, MAP2K4, MAP2K6, MAP2K7, MAPK14, PEBP1, RRM1*) (Fig. 3d). As *IL11RA* expression in MDA-MB-231T was too low to be downregulated, overexpression of either IL11RA or the empty vector was performed in MCF7 cell line (Fig. 4d). The two IL11RA overexpressing clones, #2 and 3, showed a 2.1-(*p*=0.0008) and 1.4-(*p*=0.04) fold increase in cell migration as compared to the vector expressing cells. The overexpression of IL11RA in the MCF7 induced a reduction in cell proliferation at a 72 h time point (*p*=0.03 and 0.01) as compared the control sample (Vector 1) (Supplementary Fig. 4d).

In the microarray analysis, *PDE5A* (phosphodiesterase-5A), the gene encoding for the enzyme involved in the regulation of cGMP [50], was upregulated at 48 h (t-stat=1.99, *p*=0.05) and at 96 h (t-stat=4.77, *p*<0.001) from siRNA-MSG transfection (Table 1). The qRT-PCR validation showed at least a 1.5-fold PDE5A upregulation by knockdown of eight MSGs (*ARHGDIB, BRMS1, CASP8, CD44, CDH2, MAP2K4, MAPK14, PEBP1*) (Fig. 3e). Two shRNA sequences silenced PDE5A expression in MDA-MB-231T cells, creating stable clones #43 and #45 (Fig. 4e). Both shPDE5A_43 and shPDE5A_45 clones with silenced PDE5A expression showed a significant reduction in cell migration (47 %, *p*=0.01 and 66 %, *p*=0.005, respectively) as compared to the shRNA negative control (NT). No difference in cell proliferation was observed between the stable clones as compared to either the empty vector (pLKO)- or scramble-shRNA transfectants (Supplementary Fig. 4e). To further investigate the inverse association of *PDE5A* expression with metastatic property, PDE5A protein levels were measured in BT474 cells and a metastatic sub-clone BT474-M1

[40]. PDE5A expression was higher in the highly metastatic BT474-M1 cells than in the low metastatic BT474 cell line (Supplementary Fig. 5).

In summary, using microarray analysis and qRT-PCR, we identified and validated several candidate genes whose expression was inversely associated to multiple MSGs in the breast cancer cell line, MCF7. The *in vitro* data demonstrate that the selected candidates, DNM3, OAS1, UGT1A, IL11RA and PDE5A, were able to affect cell migration to various degrees when silenced (DNM3, OAS1, UGT1A, PDE5A) or overexpressed (IL11RA) in metastatic breast cancer cells. The data demonstrate that common downstream signaling pathways link multiple MSGs. Many of these common networks are either new, or not well studied in the metastasis field. The data also provide a first comprehensive gene expression analysis upon MSGs downregulation. PDE5A, being a known druggable target [51], was selected for further investigation.

PDE5A downregulation reduced metastasis formation in a mouse experimental metastasis model

To investigate the role of PDE5A in metastasis formation *in vivo*, MDA-MB-231T breast cancer cells expressing shRNA-PDE5A (clone#43 and #45), empty vector or negative control shRNA were injected into tail veins of athymic nude mice. Nine weeks post-injection, the lungs were collected and fixed in Bouin's solution. Metastases visible on the surface of the lungs were counted (Fig. 5a). Both PDE5A silenced clones reduced metastasis (clone#43 median= 15, p=0.0006 and clone#45 median= 42, p=0.043) as compared to the control sample (median= 64.5), which included both the empty vector and shRNA-negative cells. The lungs were then paraffin-embedded and sectioned for further analysis. H&E staining confirmed that the number of lung metastases in both shPDE5A_43 (median=14.5, *p*=0.009) and shPDE5A_45 (median=20.2, *p*=0.045) samples was significantly reduced when compared to the control sample (median=38) (Fig. 5b, c). To assure that the observed phenotype was a result of a direct influence on the metastatic process rather than an effect on the growth rate of the cells, cell proliferation was measured in the lung metastatic lesions using Ki67 staining (Fig. 5d, e). No difference in the number of Ki67-positive cells was observed in the metastatic lesions between the experimental groups. The data show that PDE5A, inversely associated to eight MSGs at 96 h of siRNA-MSG transfection, functionally participated in cell motility *in vitro* and metastasis *in vivo*.

Validation of inverse correlation between PDE5A and 8 MSGs in human breast cancer cohorts

The inverse association between *PDE5A* and the identified MSGs was further validated in two human breast cancer gene expression cohorts: GSE2034 and GSE1456 [41, 42]. The datasets included 286 and 159 breast carcinoma samples, respectively. Partek Genomics Suite was used to evaluate the correlation in terms of expression of *PDE5A* with the set of 8 MSGs (*ARHGDIB*, *BRMS1*, *CASP8*, *CD44*, *CDH2*, *MAP2K4*, *MAPK14*, *PEBP1).* The mean expression value for the probe set of each gene was plotted in a bar graph for each dataset (Fig. 6). When *PDE5A* expression was compared to the MSGs, *PDE5A* was significantly inversely correlated to the 8 identified MSGs in both human breast cancer cohorts (*p*=0.003 in GSE2034 and *p*=0.03 in GSE1456; Table 3).

The association between *DNM3*, *IL11RA*, *OAS1*, *UGT1A* and their respective inversely expressed MSGs was also investigated in the same human breast cancer cohorts. DNM3 expression showed a significant inverse correlation to its MSGs set (*CASP8*, *CD44*, *CD82*, *CDH1*, *DRG1*, *GSN*, *MAP2K4*) with $p=0.02$ in both breast cancer cohorts. *UGT1A* and *OAS1* showed a trend toward an inverse correlation to their respective MSGs sets, while no significant correlation was found for *IL11RA* and its MSGs set (Table 3).

A third human breast cancer gene expression cohort (GSE26304) was used to perform Pearson correlation coefficient analysis for PDE5A. This dataset includes 115 samples with different stages of breast cancer (31 pure DCIS patients, 36 IDC patients, 42 mixed and 6 normal) and is thus suited for this analysis. PDE5A showed an inverse correlation to all of 8 MSGs included in the analysis (Table 4).

Discussion

It has been argued that the metastatic process, in contrast to conventional wisdom, is a ripe target for therapeutic development, as it widely contributes to cancer patients' deaths [52], although new clinical trial designs will be needed for validation [53, 54]. Multiple MSGs have been discovered in model systems. Through apparently different pathways, based on the gene-by-gene literature, they lead to the same biological event: suppression of metastasis formation. Since suppressor genes are virtually impossible to directly and uniformly deliver, we and others have focused on downstream pathways, herein transcripts with opposite, presumed pro-metastatic expression patterns. We present the first comprehensive analysis of the downstream transcriptional effects of MSG expression, and identify several common gene expression pathways of functional and potential therapeutic significance.

Nineteen MSGs were transiently downregulated, each by two siRNAs at two tissue culture time points in MCF7 breast carcinoma cells. MCF7 cells were chosen as a line expressing relatively high levels of 10 of the 19 genes and, consistent with high MSG expression, exhibit ing a relatively low tumor cell motility phenotype. While a good system for this analysis, not all of the MSGs have been validated as functional in this line, and the transcriptional analysis was conducted on tissue culture plastic, which may vary from *in vivo* patterns. The two siRNAs sometimes failed to knock down gene expression to identical levels. Despite these caveats, and using a simple bioinformatics process, several upregulated genes were identified comparing the gene expression profile of siRNA-MSGs and the control samples. Inversely related genes were chosen on the basis of their upregulation in five or more siRNA-MSGs, t-statistic and p-value (p<0.01). Many of the remaining genes had interesting but less statistically significant gene expression trends, suggesting that their transcriptional effects may still be of interest. The raw gene expression data can be used for additional, potentially more sophisticated analyses of MSGs function.

Our analysis identified 257 genes at 48 h and 419 genes at 96 h inversely associated with multiple MSGs expression. Ingenuity Pathway analysis showed that six major pathways were affected by multiple MSGs silencing: cell morphology, proliferation, metabolism, development, cell signaling and immune signaling. Eighteen genes were chosen for validation by qRT-PCR using independent cultures. Functional experiments were conducted

in an independent cell line, MDA-MB-231T, to test the generality of the observations. Several of the identified genes, or their gene families, have been recognized in the metastasis literature. The current analysis suggests the widespread relevance of these genes to metastasis via their transcriptional regulation by multiple MSGs. Other genes were new to the metastasis literature.

The dynamin family is involved in membrane trafficking processes such as vesicle scission at the plasma membrane or trans-Golgi network, phagocytosis, cytokinesis, podosome formation, and endocytosis [47, 55–59]. DNM2 upregulation has been linked to increased motility and metastasis in a pancreatic model system [58], and inhibitors have been identified [60]. DNM3 is normally expressed in neurons, testis and megakaryocytes. Little is known about a role of DNM3 in cancer. Herein we demonstrate a trend of reduced tumor cell motility *in vitro* when DNM3 was inhibited by shRNAs in metastatic MDA-MB-231T cells.

Similarly, 2α-5α-Oligoadenylate Synthetase-1 (*OAS1*) encodes a well characterized enzyme involved in the innate immune response to viral infection [48]. After its induction by interferons, OAS1 activates RNase L, which degrades viral and cellular RNA and inhibits replication and protein synthesis suppressing viral growth and promoting apoptosis [61]. The only link of *OAS1* to cancer is found in polymorphisms associated with prostate cancer [62, 63]. Herein, downregulation of OAS1 by two shRNAs in MDA-MB-231T cells resulted in a trend of decreased cell motility *in vitro*. The partial effects of gene knockdown on tumor cell motility may deserve additional experimentation as they were interrogated in only one cell line and may have significant combinatorial effects.

The *IL11RA* gene encodes the α-subunit that, together with gp130, forms the receptor for the cytokine IL11, a member of the IL-6 family. Its activation induces JAK-STAT and MAPK signaling cascades [49]. IL11Rα expression was associated with tumor progression in prostate, ovarian, gastric, hepatocellular and breast cancers, and with tumor invasion and lymphatic infiltration in colorectal carcinomas [64–67]. Herein, overexpression of IL11RA significantly increased tumor cell motility *in vitro* and exerted limited effects on proliferation of MCF7 cells. It should be pointed out that these last two candidates are both involved in the immune response. Immune signaling was a major pathway affected by MSGs silencing.

In contrast to these genes, the identification of *UGT1A* transcripts as being both inversely expressed with multiple MSGs and functionally contributory to motility is, to our knowledge, completely unexpected. UDP-glucoronosyltransferases are membrane-bound enzymes, localized in the endoplasmatic reticulum, that catalyze the glucoronidation of various endogenous and exogenous compounds such as bilirubin, bile acids, steroid hormones, chemotherapeutics, non-steroidal anti-inflammatory drugs, anticonvulsants. Eighteen *UGT* transcripts have been identified and divided in three families UGT1A, UGT2A and UGT2B based upon sequence homology [68]. The UGT1 family includes nine functional proteins (A1, A3-10) and four pseudogenes derived from alternative splicing of a single gene locus [69]. The several *UGT1A* isoforms show different tissue expression patterns, with only *UGT1A9* localized in breast [46]. Several members of the UGT1A

family, such as UGT1A1 and UGT1A9, are involved in the conjugation of estradiol and its hydroxylated and/or methylated metabolites [70]. Polymorphic variants of UGT1A1 and UGT1A9, highly expressed in liver, have been widely studied for their influence on irinotecan metabolism and toxicity [71, 72]. Although UGT1A polymorphisms and their functional consequences appear to play important role in cancer risk and response to therapy, their direct influence in cancer progression remains to be characterized. Herein we demonstrate that the downregulation of both UGT1A isoforms, *UGT1A1* and *UGT1A9*, in the ER-negative, metastatic cell line MDA-MB-231T resulted in reduced cell motility, suggesting a potential role in this process.

A functional role for *PDE5A* (Phosphodiesterase type-5A), which was inversely associated with 8 MSGs, was tested both in motility assays and in an *in vivo* metastasis assay. In addition, the inverse correlation of *PDE5A* and the 8 MSGs (*ARHGDIB*, *BRMS1*, *CASP8*, *CD44*, *CDH2*, *MAP2K4*, *MAPK14*, *PEBP1*) was validated in three human breast cancer cohorts. The datasets included microarray data from primary tumor samples, and the expression of *PDE5A* was very low. It would be interesting to analyze potential inverse correlation in metastatic biopsies in the future, where we expect a reduction in expression of the MSG and a consequent increase in *PDE5A* expression.

Phosphodiesterases are intracellular enzymes that hydrolyze cyclic adenosine and guanosine monophosphates (cAMP and cGMP) to their respective 5′-nucleoside monophosphate. There are 11 PDE families with different substrate specificities, regulatory properties, tissue localizations, and inhibitor sensitivities (reviewed in [73, 74]). Through alternative splicing, the *PDE5A* gene generates three PDE5 isoforms, PDE5A1-3 [73]. PDE5 is a cyclic guanosine monophosphate (cGMP)-specific phosphodiesterase [50], involved in regulation of apoptosis [75–77], synaptic plasticity [78], platelet aggregation [79], and fluid secretion in intestinal cells [80]. PDE5 inhibitors, sildenafil (Viagra®) and vardenafil (Levitra®) are FDA-approved drugs used for erectile dysfunction [51, 81]. In preclinical experiments they increase chemotherapeutic sensitivity to many, but not all drugs tested [82–87]. A role for PDE5 or its pharmacologic inhibitors in metastasis has been reported in lung colonization by melanoma cells [88]. Herein, PDE5A was described for the first time as a downstream target of multiple MSGs. PDE5A downregulation in metastatic breast cancer cells resulted in reduced cell motility and lung metastasis formation in experimental metastatic models. Although cGMP is an important second messenger in cell signaling, how PDE5A modulates signaling pathways in the context of metastasis in still unclear and should be a topic of further investigation.

How the MSGs regulate PDE5A expression is another question of interest. Ingenuity pathway analysis of PDE5A and the 8 inversely correlated MSGs suggested a functional connection between PDE5A and MSGs mediated by PP1-C (protein phosphatase 1) and IL1β (interleukin 1beta) ([89, 90] and data not shown). Although lacking significant p-values, both PP1-C and IL1β were also present in our MCF7 microarray dataset, with PP1-C being downregulated (48 h: t-stat=−0.72, p=0.47; 96 h: t-stat=−1.47, p=0.14) and IL1β upregulated (48 h: t-stat=1.91, p=0.06; 96 h: t-stat=1.51, p=0.14). The data suggest an indirect regulatory effect on PDE5A by MSGs, mediated by PP1-C and IL1β.

The data demonstrated only a partial (47–62%) reduction in metastasis formation by downregulation of PDE5A, suggesting that the anti-metastatic effects of multiple MSGs may be mediated by multiple factors/pathways. It would be interesting to evaluate the metastatic properties of tumor cells upon knocking down the expression of a combination of the inversely correlated genes identified in this study. In summary, the data suggest that genes inversely correlated to multiple MSGs may contribute to tumor cell migration and may represent the new focus in the investigation of metastasis-related pathways.

Supplementary Material

Refer to Web version on PubMed Central for supplementary material.

Acknowledgments

Abbreviations

MSGs	metastasis suppressor genes
PDE5A	phosphodiesterase 5A
UGT1A	UPD-glucoronosyltransferase 1 A family
H&E	hematoxylin and eosin
IL11RA	interleukin-11 receptor alpha
DNM3	dynamin-3
OAS1	$2'$-$5'$-oligoadenylate synthetase-1
FBS	Fetal bovine serum
siRNA	Small interfering RNA
shRNA	Small hairpin RNA

References

1. DeSantis C, et al. Breast cancer statistics, 2013. CA: a cancer journal for clinicians. 2014; 64(1):52–62. [PubMed: 24114568]

2. Siegel R, Naishadham D, Jemal A. Cancer statistics, 2013. CA: a cancer journal for clinicians. 2013; 63(1):11–30. [PubMed: 23335087]

3. Eccles SA, Welch DR. Metastasis: recent discoveries and novel treatment strategies. Lancet. 2007; 369(9574):1742–57. [PubMed: 17512859]

4. Stafford LJ, Vaidya KS, Welch DR. Metastasis suppressors genes in cancer. The international journal of biochemistry & cell biology. 2008; 40(5):874–91. [PubMed: 18280770]

5. Steeg PS, et al. Altered expression of NM23, a gene associated with low tumor metastatic potential, during adenovirus 2 Ela inhibition of experimental metastasis. Cancer research. 1988; 48(22):6550–4. [PubMed: 2460224]

6. Sleeman J, Steeg PS. Cancer metastasis as a therapeutic target. European journal of cancer. 2010; 46(7):1177–80. [PubMed: 20307970]

7. Berger JC, et al. Metastasis suppressor genes: from gene identification to protein function and regulation. Cancer biology & therapy. 2005; 4(8):805–12. [PubMed: 16082183]

8. Samant RS, et al. Breast cancer metastasis suppressor 1 (BRMS1) inhibits osteopontin transcription by abrogating NF-kappaB activation. Molecular cancer. 2007; 6:6. [PubMed: 17227585]

9. Smith SC, Theodorescu D. Learning therapeutic lessons from metastasis suppressor proteins. Nature reviews Cancer. 2009; 9(4):253–64. [PubMed: 19242414]

10. Palmieri D, et al. Medroxyprogesterone acetate elevation of Nm23-H1 metastasis suppressor expression in hormone receptor-negative breast cancer. Journal of the National Cancer Institute. 2005; 97(9):632–42. [PubMed: 15870434]

11. Liu F, Qi HL, Chen HL. Effects of all-trans retinoic acid and epidermal growth factor on the expression of nm23-H1 in human hepatocarcinoma cells. Journal of cancer research and clinical oncology. 2000; 126(2):85–90. [PubMed: 10664247]

12. Mashimo T, et al. Activation of the tumor metastasis suppressor gene, KAI1, by etoposide is mediated by p53 and c-Jun genes. Biochemical and biophysical research communications. 2000; 274(2):370–6. [PubMed: 10913345]

13. El Touny LH, Banerjee PP. Genistein induces the metastasis suppressor kangai-1 which mediates its anti-invasive effects in TRAMP cancer cells. Biochemical and biophysical research communications. 2007; 361(1):169–75. [PubMed: 17658479]

14. Horak CE, et al. Nm23-H1 suppresses metastasis by inhibiting expression of the lysophosphatidic acid receptor EDG2. Cancer research. 2007; 67(24):11751–9. [PubMed: 18089805]

15. Titus B, et al. Endothelin axis is a target of the lung metastasis suppressor gene RhoGDI2. Cancer research. 2005; 65(16):7320–7. [PubMed: 16103083]

16. Horak CE, et al. Nm23-H1 suppresses tumor cell motility by down-regulating the lysophosphatidic acid receptor EDG2. Cancer research. 2007; 67(15):7238–46. [PubMed: 17671192]

17. Marshall JC, et al. Effect of inhibition of the lysophosphatidic acid receptor 1 on metastasis and metastatic dormancy in breast cancer. Journal of the National Cancer Institute. 2012; 104(17):1306–19. [PubMed: 22911670]

18. Minn AJ, et al. Identification of novel metastasis suppressor signaling pathways for breast cancer. Cell cycle. 2012; 11(13):2452–7. [PubMed: 22659842]

19. Yun J, et al. Signalling pathway for RKIP and Let-7 regulates and predicts metastatic breast cancer. The EMBO journal. 2011; 30(21):4500–14. [PubMed: 21873975]

20. Xia W, et al. The Src-suppressed C kinase substrate, SSeCKS, is a potential metastasis inhibitor in prostate cancer. Cancer research. 2001; 61(14):5644–51. [PubMed: 11454719]

21. Theodorescu D, et al. Reduced expression of metastasis suppressor RhoGDI2 is associated with decreased survival for patients with bladder cancer. Clinical cancer research : an official journal of the American Association for Cancer Research. 2004; 10(11):3800–6. [PubMed: 15173088]

22. Phadke PA, et al. BRMS1 suppresses breast cancer experimental metastasis to multiple organs by inhibiting several steps of the metastatic process. The American journal of pathology. 2008; 172(3):809–17. [PubMed: 18276787]

23. Stupack DG, et al. Potentiation of neuroblastoma metastasis by loss of caspase-8. Nature. 2006; 439(7072):95–9. [PubMed: 16397500]

24. Rudy W, et al. The two major CD44 proteins expressed on a metastatic rat tumor cell line are derived from different splice variants: each one individually suffices to confer metastatic behavior. Cancer research. 1993; 53(6):1262–8. [PubMed: 8443806]

25. Kallakury BV, et al. Decreased levels of CD44 protein and mRNA in prostate carcinoma. Correlation with tumor grade and ploidy. Cancer. 1996; 78(7):1461–9. [PubMed: 8839552]

26. Phillips KK, et al. Correlation between reduction of metastasis in the MDA-MB-435 model system and increased expression of the Kai-1 protein. Molecular carcinogenesis. 1998; 21(2):111–20. [PubMed: 9496911]

27. Yang X, et al. KAI1, a putative marker for metastatic potential in human breast cancer. Cancer letters. 1997; 119(2):149–55. [PubMed: 9570365]

28. Perl AK, et al. A causal role for E-cadherin in the transition from adenoma to carcinoma. Nature. 1998; 392(6672):190–3. [PubMed: 9515965]

29. Frixen UH, et al. E-cadherin-mediated cell-cell adhesion prevents invasiveness of human carcinoma cells. The Journal of cell biology. 1991; 113(1):173–85. [PubMed: 2007622]

30. Kashima T, et al. Overexpression of cadherins suppresses pulmonary metastasis of osteosarcoma in vivo. International journal of cancer Journal international du cancer. 2003; 104(2):147–54. [PubMed: 12569568]

31. Nakajima G, et al. CDH11 expression is associated with survival in patients with osteosarcoma. Cancer genomics & proteomics. 2008; 5(1):37–42. [PubMed: 18359978]

32. Guan RJ, et al. Drg-1 as a differentiation-related, putative metastatic suppressor gene in human colon cancer. Cancer research. 2000; 60(3):749–55. [PubMed: 10676663]

33. Fujita H, et al. Gelsolin functions as a metastasis suppressor in B16-BL6 mouse melanoma cells and requirement of the carboxyl-terminus for its effect. International journal of cancer Journal international du cancer. 2001; 93(6):773–80. [PubMed: 11519036]

34. Beck BH, Welch DR. The KISS1 metastasis suppressor: a good night kiss for disseminated cancer cells. European journal of cancer. 2010; 46(7):1283–9. [PubMed: 20303258]

35. Yamada SD, et al. Mitogen-activated protein kinase kinase 4 (MKK4) acts as a metastasis suppressor gene in human ovarian carcinoma. Cancer research. 2002; 62(22):6717–23. [PubMed: 12438272]

36. Hickson JA, et al. The p38 kinases MKK4 and MKK6 suppress metastatic colonization in human ovarian carcinoma. Cancer research. 2006; 66(4):2264–70. [PubMed: 16489030]

37. Vander Griend DJ, et al. Suppression of metastatic colonization by the context-dependent activation of the c-Jun NH2-terminal kinase kinases JNKK1/MKK4 and MKK7. Cancer research. 2005; 65(23):10984–91. [PubMed: 16322247]

38. Hagan S, et al. Reduction of Raf-1 kinase inhibitor protein expression correlates with breast cancer metastasis. Clinical cancer research : an official journal of the American Association for Cancer Research. 2005; 11(20):7392–7. [PubMed: 16243812]

39. Gautam A, Bepler G. Suppression of lung tumor formation by the regulatory subunit of ribonucleotide reductase. Cancer research. 2006; 66(13):6497–502. [PubMed: 16818620]

40. Beyer I, et al. Controlled extracellular matrix degradation in breast cancer tumors improves therapy by trastuzumab. Molecular therapy : the journal of the American Society of Gene Therapy. 2011; 19(3):479–89. [PubMed: 21081901]

41. Wang Y, et al. Gene-expression profiles to predict distant metastasis of lymph-node-negative primary breast cancer. Lancet. 2005; 365(9460):671–9. [PubMed: 15721472]

42. Pawitan Y, et al. Gene expression profiling spares early breast cancer patients from adjuvant therapy: derived and validated in two population-based cohorts. Breast cancer research : BCR. 2005; 7(6):R953–64. [PubMed: 16280042]

43. Muggerud AA, et al. Molecular diversity in ductal carcinoma in situ (DCIS) and early invasive breast cancer. Molecular oncology. 2010; 4(4):357–68. [PubMed: 20663721]

44. Guillemette C, et al. UGT genomic diversity: beyond gene duplication. Drug metabolism reviews. 2010; 42(1):24–44. [PubMed: 19857043]

45. Guillemette C, et al. Genetic polymorphisms in uridine diphospho-glucuronosyltransferase 1A1 and association with breast cancer among African Americans. Cancer research. 2000; 60(4):950–6. [PubMed: 10706110]

46. Albert C, et al. The monkey and human uridine diphosphate-glucuronosyltransferase UGT1A9, expressed in steroid target tissues, are estrogen-conjugating enzymes. Endocrinology. 1999; 140(7):3292–302. [PubMed: 10385426]

47. Okamoto PM, Herskovits JS, Vallee RB. Role of the basic, proline-rich region of dynamin in Src homology 3 domain binding and endocytosis. The Journal of biological chemistry. 1997; 272(17): 11629–35. [PubMed: 9111080]

48. Justesen J, Hartmann R, Kjeldgaard NO. Gene structure and function of the 2′-5′-oligoadenylate synthetase family. Cellular and molecular life sciences : CMLS. 2000; 57(11):1593–612. [PubMed: 11092454]

49. Taga T, Kishimoto T. Gp130 and the interleukin-6 family of cytokines. Annual review of immunology. 1997; 15:797–819.

50. Juilfs DM, et al. Cyclic GMP as substrate and regulator of cyclic nucleotide phosphodiesterases (PDEs). Reviews of physiology, biochemistry and pharmacology. 1999; 135:67–104.

51. Boolell M, et al. Sildenafil: an orally active type 5 cyclic GMP-specific phosphodiesterase inhibitor for the treatment of penile erectile dysfunction. International journal of impotence research. 1996; 8(2):47–52. [PubMed: 8858389]

52. Weber GF. Why does cancer therapy lack effective anti-metastasis drugs? Cancer letters. 2013; 328(2):207–11. [PubMed: 23059758]

53. Brabletz T, et al. Roadblocks to translational advances on metastasis research. Nature medicine. 2013; 19(9):1104–9.

54. Steeg PS. Perspective: The right trials. Nature. 2012; 485(7400):S58–9. [PubMed: 22648501]

55. Perrais D, Merrifield CJ. Dynamics of endocytic vesicle creation. Developmental cell. 2005; 9(5): 581–92. [PubMed: 16256734]

56. Ochoa GC, et al. A functional link between dynamin and the actin cytoskeleton at podosomes. The Journal of cell biology. 2000; 150(2):377–89. [PubMed: 10908579]

57. Gold ES, et al. Dynamin 2 is required for phagocytosis in macrophages. The Journal of experimental medicine. 1999; 190(12):1849–56. [PubMed: 10601359]

58. Kruchten AE, McNiven MA. Dynamin as a mover and pincher during cell migration and invasion. Journal of cell science. 2006; 119(Pt 9):1683–90. [PubMed: 16636070]

59. Thompson HM, et al. The large GTPase dynamin associates with the spindle midzone and is required for cytokinesis. Current biology : CB. 2002; 12(24):2111–7. [PubMed: 12498685]

60. Harper CB, et al. Targeting membrane trafficking in infection prophylaxis: dynamin inhibitors. Trends in cell biology. 2013; 23(2):90–101. [PubMed: 23164733]

61. Domingo-Gil E, Esteban M. Role of mitochondria in apoptosis induced by the 2–5A system and mechanisms involved. Apoptosis : an international journal on programmed cell death. 2006; 11(5): 725–38. [PubMed: 16532271]

62. Mandal S, Abebe F, Chaudhary J. 2′-5′ oligoadenylate synthetase 1 polymorphism is associated with prostate cancer. Cancer. 2011; 117(24):5509–18. [PubMed: 21638280]

63. Kazma R, et al. Association of the innate immunity and inflammation pathway with advanced prostate cancer risk. PloS one. 2012; 7(12):e51680. [PubMed: 23272139]

64. Campbell CL, et al. Increased expression of the interleukin-11 receptor and evidence of STAT3 activation in prostate carcinoma. The American journal of pathology. 2001; 158(1):25–32. [PubMed: 11141475]

65. Campbell CL, et al. Interleukin-11 receptor expression in primary ovarian carcinomas. Gynecologic oncology. 2001; 80(2):121–7. [PubMed: 11161848]

66. Hanavadi S, et al. Expression of interleukin 11 and its receptor and their prognostic value in human breast cancer. Annals of surgical oncology. 2006; 13(6):802–8. [PubMed: 16614887]

67. Yoshizaki A, et al. Expression of interleukin (IL)-11 and IL-11 receptor in human colorectal adenocarcinoma: IL-11 up-regulation of the invasive and proliferative activity of human colorectal carcinoma cells. International journal of oncology. 2006; 29(4):869–76. [PubMed: 16964382]

68. Mackenzie PI, et al. Nomenclature update for the mammalian UDP glycosyltransferase (UGT) gene superfamily. Pharmacogenetics and genomics. 2005; 15(10):677–85. [PubMed: 16141793]

69. Gong QH, et al. Thirteen UDPglucuronosyltransferase genes are encoded at the human UGT1 gene complex locus. Pharmacogenetics. 2001; 11(4):357–68. [PubMed: 11434514]

70. Lepine J, et al. Specificity and regioselectivity of the conjugation of estradiol, estrone, and their catecholestrogen and methoxyestrogen metabolites by human uridine diphospho-glucuronosyltransferases expressed in endometrium. The Journal of clinical endocrinology and metabolism. 2004; 89(10):5222–32. [PubMed: 15472229]

71. Gagne JF, et al. Common human UGT1A polymorphisms and the altered metabolism of irinotecan active metabolite 7-ethyl-10-hydroxycamptothecin (SN-38). Molecular pharmacology. 2002; 62(3):608–17. [PubMed: 12181437]

72. Innocenti F, et al. Haplotypes of variants in the UDP-glucuronosyltransferase1A9 and 1A1 genes. Pharmacogenetics and genomics. 2005; 15(5):295–301. [PubMed: 15864130]

73. Lugnier C. Cyclic nucleotide phosphodiesterase (PDE) superfamily: a new target for the development of specific therapeutic agents. Pharmacology & therapeutics. 2006; 109(3):366–98. [PubMed: 16102838]

74. Maurice DH, et al. Advances in targeting cyclic nucleotide phosphodiesterases. Nature reviews Drug discovery. 2014; 13(4):290–314. [PubMed: 24687066]

75. Lim JT, et al. Sulindac derivatives inhibit growth and induce apoptosis in human prostate cancer cell lines. Biochemical pharmacology. 1999; 58(7):1097–107. [PubMed: 10484067]

76. Sarfati M, et al. Sildenafil and vardenafil, types 5 and 6 phosphodiesterase inhibitors, induce caspase-dependent apoptosis of B-chronic lymphocytic leukemia cells. Blood. 2003; 101(1):265–9. [PubMed: 12393651]

77. Zhu B, et al. Suppression of cyclic GMP-specific phosphodiesterase 5 promotes apoptosis and inhibits growth in HT29 cells. Journal of cellular biochemistry. 2005; 94(2):336–50. [PubMed: 15526282]

78. Shimizu-Albergine M, et al. Individual cerebellar Purkinje cells express different cGMP phosphodiesterases (PDEs): in vivo phosphorylation of cGMP-specific PDE (PDE5) as an indicator of cGMP-dependent protein kinase (PKG) activation. The Journal of neuroscience : the official journal of the Society for Neuroscience. 2003; 23(16):6452–9. [PubMed: 12878685]

79. Li Z, et al. A stimulatory role for cGMP-dependent protein kinase in platelet activation. Cell. 2003; 112(1):77–86. [PubMed: 12526795]

80. Sopory S, Kaur T, Visweswariah SS. The cGMP-binding, cGMP-specific phosphodiesterase (PDE5): intestinal cell expression, regulation and role in fluid secretion. Cellular signalling. 2004; 16(6):681–92. [PubMed: 15093609]

81. Stark S, et al. Vardenafil increases penile rigidity and tumescence in men with erectile dysfunction after a single oral dose. European urology. 2001; 40(2):181–8. discussion 9–90. [PubMed: 11528196]

82. Yip-Schneider MT, et al. Cell cycle effects of nonsteroidal anti-inflammatory drugs and enhanced growth inhibition in combination with gemcitabine in pancreatic carcinoma cells. The Journal of pharmacology and experimental therapeutics. 2001; 298(3):976–85. [PubMed: 11504793]

83. Pusztai L, et al. Phase I and II study of exisulind in combination with capecitabine in patients with metastatic breast cancer. Journal of clinical oncology : official journal of the American Society of Clinical Oncology. 2003; 21(18):3454–61. [PubMed: 12972520]

84. Whitehead CM, et al. Exisulind-induced apoptosis in a non-small cell lung cancer orthotopic lung tumor model augments docetaxel treatment and contributes to increased survival. Molecular cancer therapeutics. 2003; 2(5):479–88. [PubMed: 12748310]

85. Soriano AF, et al. Synergistic effects of new chemopreventive agents and conventional cytotoxic agents against human lung cancer cell lines. Cancer research. 1999; 59(24):6178–84. [PubMed: 10626810]

86. Li Q, Shu Y. Pharmacological Modulation of Cytotoxicity and Cellular Uptake of Anti-cancer Drugs by PDE5 Inhibitors in Lung Cancer Cells. Pharmaceutical research. 2013

87. Hu J, et al. Phosphodiesterase type 5 inhibitors increase Herceptin transport and treatment efficacy in mouse metastatic brain tumor models. PloS one. 2010; 5(4):e10108. [PubMed: 20419092]

88. Arozarena I, et al. Oncogenic BRAF induces melanoma cell invasion by downregulating the cGMP-specific phosphodiesterase PDE5A. Cancer cell. 2011; 19(1):45–57. [PubMed: 21215707]

89. Murthy KS. Contractile agonists attenuate cGMP levels by stimulating phosphorylation of cGMP-specific PDE5; an effect mediated by RhoA/PKC-dependent inhibition of protein phosphatase 1. British journal of pharmacology. 2008; 153(6):1214–24. [PubMed: 18204475]

90. Geng Y, et al. Cyclic GMP and cGMP-binding phosphodiesterase are required for interleukin-1-induced nitric oxide synthesis in human articular chondrocytes. The Journal of biological chemistry. 1998; 273(42):27484–91. [PubMed: 9765278]
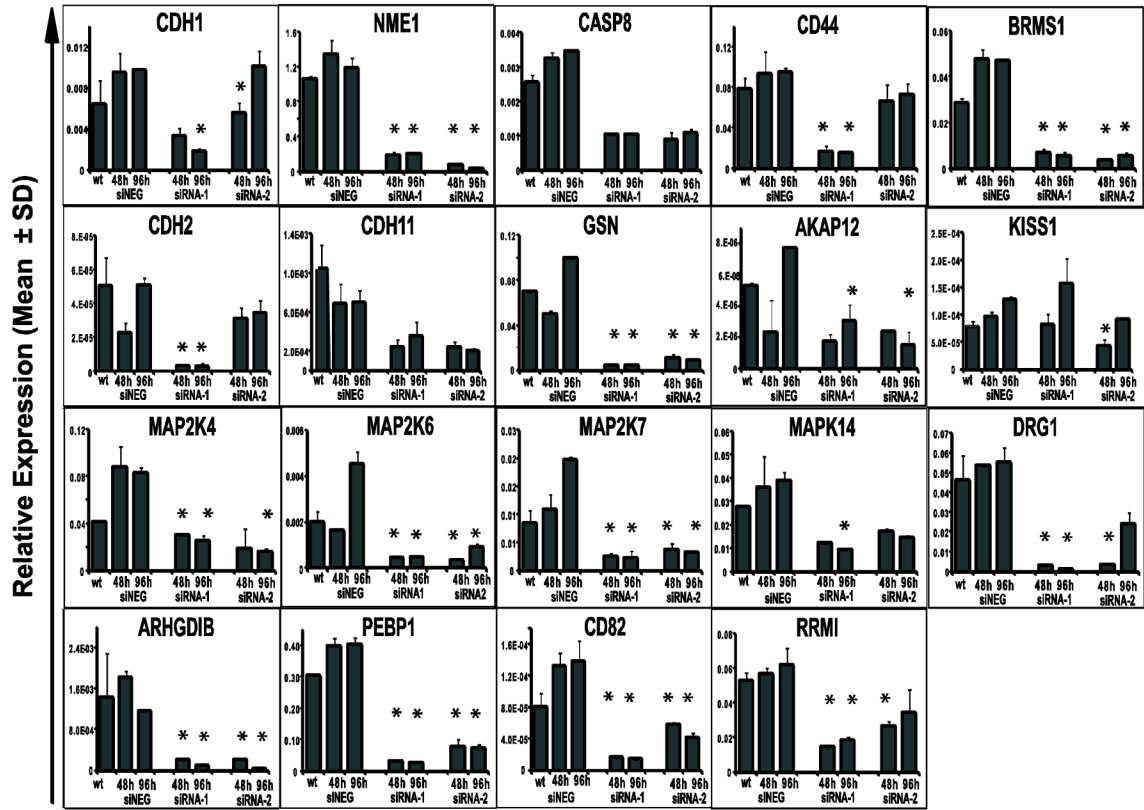
Fig. 1. Validation of the knockdown of nineteen metastasis suppressor genes (MSGs) in MCF7 breast cancer cells

Each box presents qRT-PCR data for the knockdown of one MSG, by two siRNA sequences (siRNA-1 and -2) and at two time points in culture (48 and 96 h). Y axis includes the expression of each MSG normalized to GAPDH level. Data represent the mean of triplicate experiments with SD. * p< 0.05.
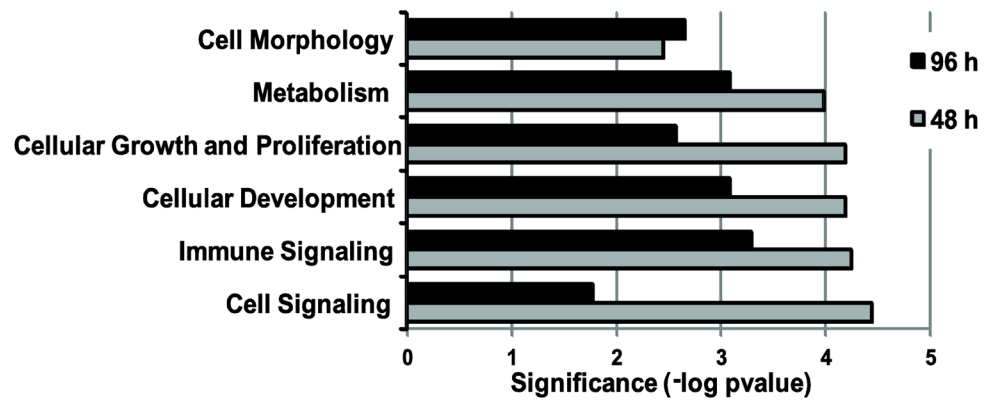
Fig. 2. Ingenuity pathway analysis of genes upregulated upon MSGs silencing in MCF7 cells
The top 6 common functions of the upregulated genes between 48 h or 96 h were identified using Ingenuity pathway analysis. The bars represent the – log *p*-value of statistical significance for each process at two time points (light grey for 48 h and dark grey for 96 h).
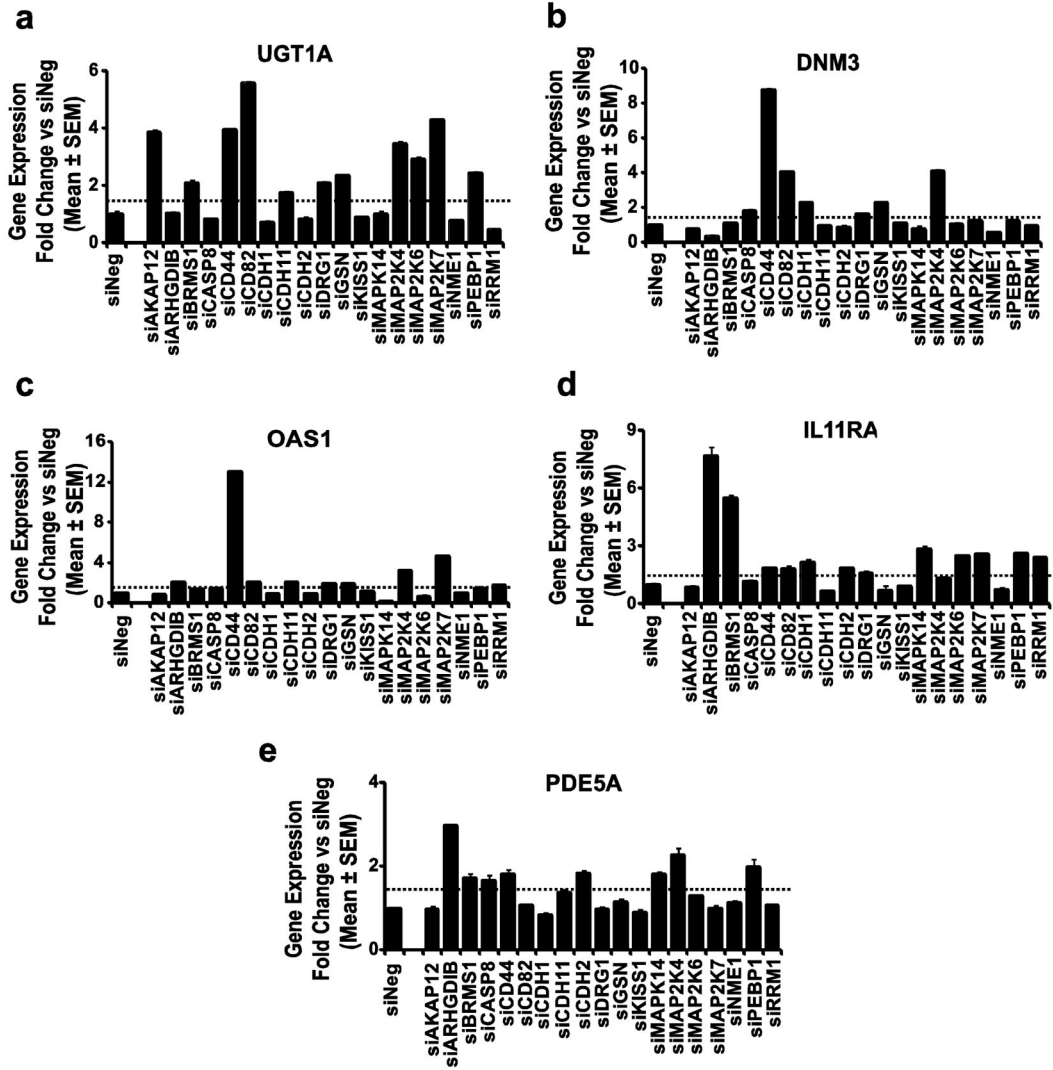
Fig. 3. Validation of inverse expression profiles of UGT1A, DNM3, OAS1, IL11RA and PDE5A in MCF7 breast cancer cells

Using an independent set of MCF7 cultures transfected with a scrambled siRNA (negative control) or siRNAs to each of 19 MSGs, qRT-PCR was performed to evaluate the expression of *UGT1A* (**a**), *DNM3* (**b**), *OAS1* (**c**), *IL11RA* (**d**) and *PDE5A* (**e**). The data are expressed as fold change in gene expression compared to negative control (siNeg), arbitrarily set as 1.0. The dotted line indicates 1.5-fold threshold. GAPDH was used to normalize the expression data.
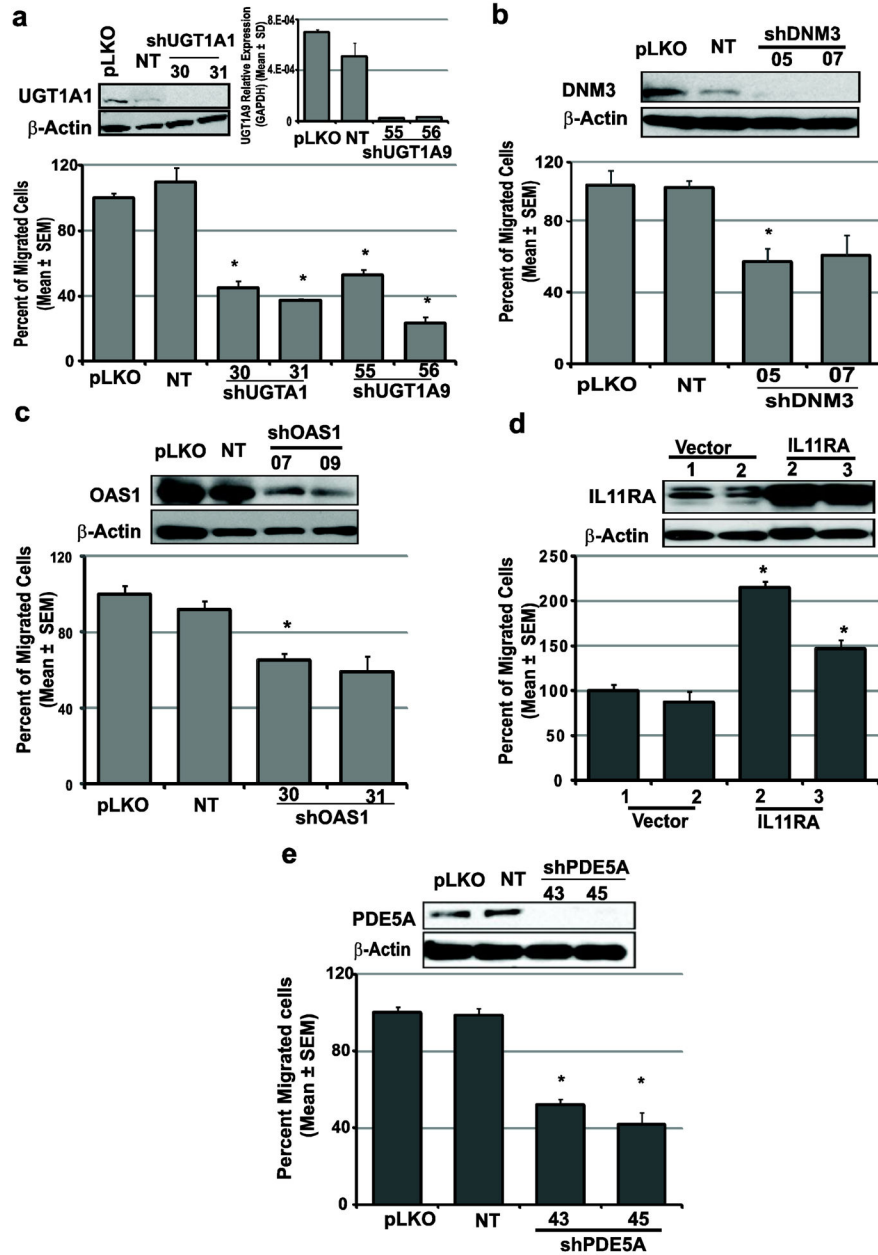
Fig. 4. UGT1A, DNM3, OAS1, IL11RA and PDE5A functionally contribute to tumor cell motility
a. Western blot or qRT-PCR was used to evaluate *UGT1A1* or *UGT1A9* expression, respectively, in MDA-MB-231T human triple negative breast carcinoma cells transfected with shRNAs to *UGT1A1* and *UGT1A9*. Controls include MDA-MB-231T cells transfected with an empty vector (pLKO) or a scrambled shRNA (NT). Below, cell motility to 1% FBS was performed, shown as the average of three independent experiments. **b–c.** Western blot analysis, followed by motility analysis was performed on MDA-MB-231T transfected with two shRNAs to *DNM3* (#05 and #07, **b**) or to *OAS1* (#07 and #09, **c**). Controls were described in a. **d.** MCF7 cells were transfected with an empty vector (clone#1 and #2) or an IL11RA construct (clone#2 and #3), and protein expression determined by western blot.

Below, motility analysis as described in **a. e.** Western blots of MDA-MB-231T cells transfected with shRNAs to *PDE5A* (#43 and #45) and *in vitro* motility of the transfected cells in Boyden chamber assays. * p< 0.05.
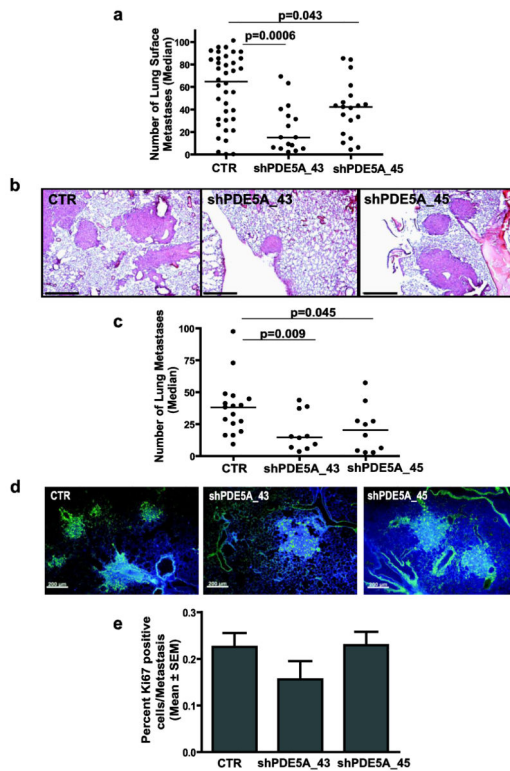
Fig. 5. PDE5A knockdown reduced *in vivo* experimental metastasis of human MDA-MB-231T breast carcinoma cells

1×10^6 MDA-MB-231T cells, transfected as described in Fig. 4 (*PDE5A* shRNAs 43 and 45 versus CTR, combined empty vector and scrambled shRNA clones), were injected into the tail veins of 6 week old athymic nude mice. **a**. Surface lung metastasis counts at necropsy, 9 weeks post-injection. Data are combined results of two experiments performed. Each dot represents a mouse, line is the median. P-values using Mann-Whitney test. **b**. Lungs were paraffin embedded for histological counts of metastases. Representative H&E stained sections are shown. Scale bar: 500 μm. **c**. Median (line) histological counts from each group. P values using Mann-Whitney test. **d**. Lung sections were stained with Ki67 (green), counterstained with DAPI (blue) to determine proliferative status. Representative images are shown. **e**. Tabulation of percentage of Ki67+ tumor cells from three sections of each mouse lung in the groups.
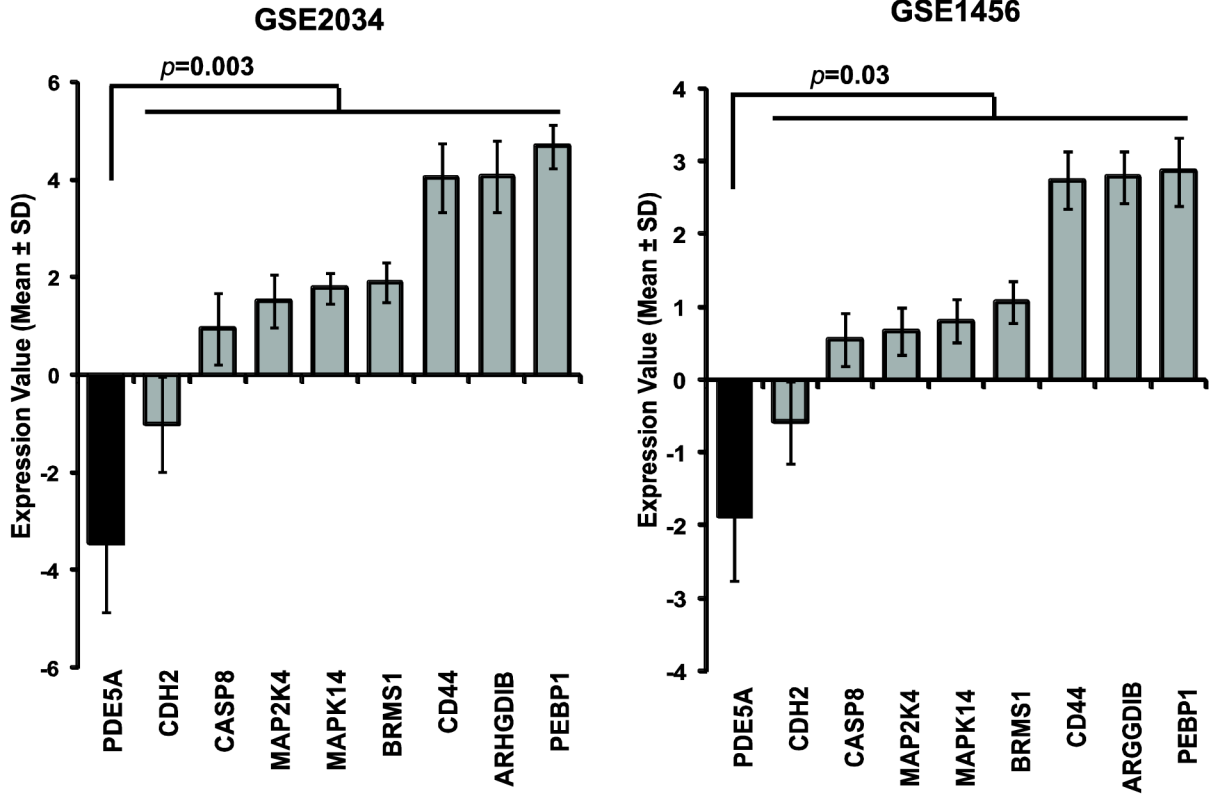
Fig. 6. PDE5A expression is inversely correlated with MSGs expression in microarray databases of human breast cancer

Expression of *PDE5A* and 8 MSGs in breast cancer cohorts was evaluated using two publicly available breast cancer datasets (GSE2034 and GSE1456). For each gene of interest, the $\log_2$-transformed expression values were averaged and plotted on a bar chart as mean ± SD. *P*-values of the correlation between *PDE5A* (dark-grey bar) and the 8 MSGs set (light-grey bars) were calculated for both datasets using the T-test statistical module on Partek Genomics Suite.

Table 1

Listing of differentially expressed genes upregulated after metastasis suppressor genes downregulation in MCF7 cell line

Affymetrix ID	RefSeq	Gene symbol	Gene name	48hr (a)		96hr (b)	
				t-statistic[#]	p-value	t-statistic[#]	p-value
1562228_s_at	NM_001083	PDE5A	Phosphodiester ase 5 A	1.99	0.05	4.77	2.7E-05
1552646_at	NM_147162	IL11RA	Interleukine 11 receptor alpha	2.18	0.04	5.69	1.5E-06
202869_at	NM_016816	OAS1	2′-5′-oligoadenylate synthetase 1	2.82	0.01	2.88	0.01
1558501_at	NM_015569	DNM3	Dynamin 3	2.52	0.01	1.06	0.29
204532_x_at	NM_021027	UGT1A	UDP glucuronosyltra nserase 1 family	2.77	0.01	0.53	0.60
205199_at	NM_001216	CA9	Carbonic anhydrase IX	1.40	0.17	3.26	2.4E-03
234514_at	NM_080823	SRMS	Src-Related Kinase Lacking C-Terminal Regulatory Tyrosine And N-Terminal	3.35	2.0E-03	0.68	0.50
1555248_a_at	NM_020922	WNK3	Myristylation Sites	4.05	2.5E-04	2.62	0.01
230854_at	NR_024050	BCAR4	Breast Cancer Anti-estrogen Resistance 4	1.14	0.26	3.93	3.5E-04
216250_s_at	NM_004811	LPXN	Leupaxin	1.02	0.32	4.94	1.6E-05
226358_at	NM_031301	APH1B	Gamma-Secretase Subunit APH-1B	1.00	0.32	3.58	9.6E-04
212977_at	NM_020311	CXCR7	Chemokine (C-X-C Motif) Receptor 7	3.24	2.5E-03	0.10	0.92
211144_x_at	NM_001003806	TARP	TCR Gamma Alternate Reading Frame Protein	3.53	1.1E-03	2.26	3.0E-02
232388_at	NM_138994	CNTNAP 4	Contactin Associated Protein-like 4	4.22	1.5E-04	2.25	3.0E-02
208166_at	NM_022564	MMP16	Matrix Metallopeptidas e 16	2.53	0.01	2.32	0.03
1561080_at	NM_182743	TXNRD1	Thioredoxin Reductase 1	3.49	1.3E-03	0.81	0.42
228391_at	NM_207352	CYP4V2	Cytochrome P450, family 4, subfamily V, polypeptide 2	3.67	7.7E-04	2.65	0.01
222900_at	NM_020645	NRIP3	Nuclear Receptor Interacting Protein 3	2.03	0.05	3.42	1.5E-03

a: NME1-1, NME1-2, CDH1-1, CDH1-2, CDH2-1, CASP8-1, CASP8-2, MAP2K4-1, MAP2K4-2, MAP2K6-1, MAP2K7-1, MAP2K7-2, MAPK14-1, MAPK14-2, CDH11-1, CDH11-2, GSN-1, GSN-2, ARHGDIB-1, ARHGDIB-2, DRG1-1, DRG1-2, CD44-1, PEBP1-1, PEBP1-2, RRM1-1, BRMS1-1, BRMS1-2, CD82-1, CD82-2.

b: NME1-1, NME1-2, CASP8-1, CASP8-2, CDH1-1, CDH2-1, CDH2-2, MAP2K4-1, MAP2K4-2, CDH11-1, CDH11-2, MAP2K6-1, MAP2K6-2, MAPK14-1, MAPK14-1, MAP2K7-1, MAP2K7-2, GSN-1, GSN-2, AKAP12-1, AKAP12-2, ARHGDIB-1, ARHGDIB-2, DRG1-1, DRG1-2, CD44-1, PEBP1-1, PEBP1-2, RRM1-1, RRM1-2, BRMS1-1, BRMS1-2, CD82-1, CD82-2.

[#] distance between the two samples in units of standard deviation

Table 2

Pathway analysis of the five selected genes in terms of biological function and pharmacological inhibition [*]

Gene name	Biological function	Drug
OAS1	Interferon signaling; recognition of bacteria and viruses	Unknown
IL11RA	Cytokine receptor; developmental process; natural killer differentiation; positive regulator of cell proliferation	Oprelvekin
DNM3	Clathrin-mediated endocitosis; remodelling of epithelian adherens junctions; megakaryocytopoiesis	Dynasore
UGT1A	Melatonin degradation; xenobiotic metabolism signaling	Rifampin, phenobarbital, beta-naphthoflavone, dexamethasone, tetrachlorodibenzodioxin, roscovitine, ritonavir, tert-butyl-hydroquinone, clotrimazol
PDE5A	cGMP-mediated signaling; proliferation; apoptosis; transdifferentiation; expression in resting tone	Aminophylline, aspirin/dipyridamole, avanafil, dipyridamole, dyphylline, nitroglycerin, pentoxifylline, sildenafil, tadalafil, theophylline, tolbutamide, udenafil, vardenafil

[*]
as reported by Ingenuity Pathway Analysis

Table 3

Inverse correlation in term of expression between candidate genes and MSGs in human breast cancer cohorts (GSE2034 and GSE1456).

	T-test *p*-value (Candidate Gene versus MSGs set)				
DATASET	**PDE5A**[a]	**DNM3**[b]	**IL11RA**[c]	**OAS1**[d]	**UGT1A**[e]
GSE2034	0.003	0.02	0.11	0.07	0.09
GSE1456	0.03	0.02	0.27	0.51	0.027

[a] inverse correlation to 8 MSGs (*ARHGDIB, BRMS1, CASP8, CD44,* CDH2, MAP2K4, MAPK14, PEBP1)

[b] inverse correlation to 7 MSGs (*CASP8, CD44, CD82, CDH1, DRG1, GSN, MAP2K4*)

[c] inverse correlation to11 MSGs (*ARHGDIB, BRMS1, CD44, CD82, CDH1, CDH2, MAPK14, MAP2K6, MAP2K7, PEBP1, RRM1*)

[d] inverse correlation to 9 MSGs (*ARHGDIB, CD44, CD82, CDH11, DRG1, GSN, MAP2K4, MAP2K7, RRM1*)

[e] inverse correlation to 11 MSGs (*AKAP12, BRMS1, CD44, CD82,* CDH11, DRG1, GSN, MAP2K4, MAP2K6, MAP2K7, PEBP1)

Table 4

Pearson correlation coefficients between PDE5A and metastasis suppressor genes in the human breast cancer cohort GSE26304.

	Correlation coefficient to PDE5A (r)[a]	p-value[b]
ARHGDIB	−0.483	2.32E−08
CD44	−0.460	1.18E−07
BRMS1	−0.440	4.31E−07
CASP8	−0.439	4.50E−07
PEBP1	−0.385	1.06E−05
MAPK14	−0.352	5.64E−05
MAP2K4	−0.317	0.0002
CDH2	−0.206	0.0136

[a]:r= Pearson 's correlation coefficient.

[b]:The P-value shown is based on a t-test focusing on negative association (alternative hypothesis: less than 0). The analysis was performed in R-package using the function cor. test.